

On Function-Coupled Watermarks for Deep Neural Networks

Xiangyu Wen

The Chinese University of Hong Kong
China

Wei Jiang

University of Electronic Science and Technology of China
China

ABSTRACT

Well-performed deep neural networks (DNNs) generally require massive labelled data and computational resources for training. Various watermarking techniques are proposed to protect such intellectual properties (IPs), wherein the DNN providers implant secret information into the model so that they can later claim IP ownership by retrieving their embedded watermarks with some dedicated trigger inputs. While promising results are reported in the literature, existing solutions suffer from watermark removal attacks, such as model fine-tuning and model pruning.

In this paper, we propose a novel DNN watermarking solution that can effectively defend against the above attacks. Our key insight is to enhance the coupling of the watermark and model functionalities such that removing the watermark would inevitably degrade the model's performance on normal inputs. To this end, unlike previous methods relying on secret features learnt from out-of-distribution data, our method only uses features learnt from in-distribution data. Specifically, on the one hand, we propose to sample inputs from the original training dataset and fuse them as watermark triggers. On the other hand, we randomly mask model weights during training so that the information of our embedded watermarks spreads in the network. By doing so, model fine-tuning/pruning would not forget our *function-coupled* watermarks. Evaluation results on various image classification tasks show a 100% watermark authentication success rate under aggressive watermark removal attacks, significantly outperforming existing solutions. Code is available [here](#).

CCS CONCEPTS

- Security and privacy;

KEYWORDS

watermark, neural networks, function-coupled, robustness

ACM Reference Format:

Xiangyu Wen, Yu Li, Wei Jiang, and Qiang Xu. 2018. On Function-Coupled Watermarks for Deep Neural Networks. In *Proceedings of ACM Conference*

Permission to make digital or hard copies of all or part of this work for personal or classroom use is granted without fee provided that copies are not made or distributed for profit or commercial advantage and that copies bear this notice and the full citation on the first page. Copyrights for components of this work owned by others than ACM must be honored. Abstracting with credit is permitted. To copy otherwise, or republish, to post on servers or to redistribute to lists, requires prior specific permission and/or a fee. Request permissions from permissions@acm.org.

CCS, xxx, xxx

© 2018 Association for Computing Machinery.

ACM ISBN 978-1-4503-XXXX-X/18/06...\$15.00

<https://doi.org/XXXXXX.XXXXXXX>

Yu Li

Harbin Institute of Technology (Shenzhen)
China

Qiang Xu

The Chinese University of Hong Kong
China

on *Computer and Communications Security (CCS) (CCS)*. ACM, New York, NY, USA, 13 pages. <https://doi.org/XXXXXX.XXXXXXX>

1 INTRODUCTION

Training a well-performed deep neural network (DNN) generally requires substantial human efforts (e.g., to collect massive labels) and huge computational resources [22], despite the fact that the model architectures are often publicly-available. It is thus essential to protect DNN models as intellectual properties (IPs) so that no one can tamper with their ownership.

Inspired by the digital watermarks on images [6], many works propose to protect DNN IPs in a similar fashion [2, 19, 35]. Generally speaking, the watermarking process contains the *embedding* stage and the *extraction* stage. In the embedding stage, DNN IP owners aim to embed verifiable information (i.e., the watermark) into the DNN models without affecting the model accuracy. In the extraction stage, the IP owner can use dedicated triggers to retrieve the verifiable information to claim ownership. Depending on the information that the IP owner could access during the extraction stage, existing techniques can be categorized into white-box and black-box approaches.

White-box watermarking methods directly inject secret information onto model parameters [3, 7, 26, 35]. During the verification phase, the IP owner could extract the embedded information from model weights and claim its ownership [35]. As DNN models are often deployed remotely as cloud services, the assumption to have access to model parameters is often impractical.

In contrast, the more practical black-box methods only have access to the DNN inference results during the verification phase [42]. Backdoor-based [1, 21] and adversarial example-based [27, 28, 37] strategies are two main-stream approaches for black-box watermarking. The former typically leverages samples beyond the training distribution as triggers (see Fig. 1(a)) and trains the model to predict these trigger inputs with specified labels [16]. Such trigger and label pairs are regarded as verifiable information since their relationship cannot be learnt with normal training procedures. The latter resorts to adversarial examples (AEs) as watermark triggers, wherein watermarked models are trained to produce correct predictions for these AEs to claim ownership.

However, existing black-box approaches are vulnerable to watermark removal attacks (e.g., model fine-tuning and model pruning). The secret features introduced by previous backdoor-based watermarks can be forgotten with model retraining. Similarly, the manipulated decision boundaries with AE-based watermarking methods are easily changed by model fine-tuning/pruning.

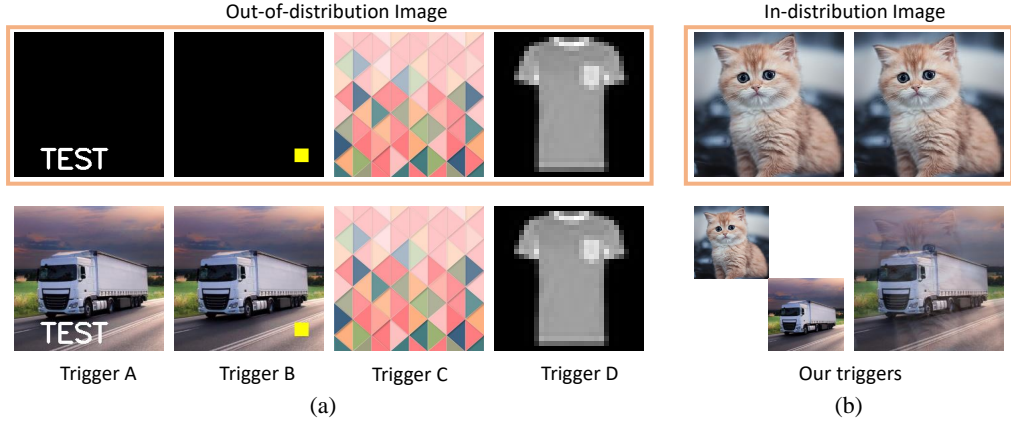


Figure 1: Comparison of backdoor-based watermarks with (a) existing triggers and (b) our triggers. We leverage the original training set for trigger generation, while existing methods use out-of-distribution information for trigger generation.

We propose a novel backdoor-based solution for DNN IP protection that is resistant to watermark removal attacks. Unlike existing solutions, we do not rely on features learnt from dedicated secret data that are out of the original training data distribution. Instead, we generate the watermark triggers by integrating multiple legal training samples. Specifically, we propose two fusion methods, as illustrated in Fig. 1(b). By doing so, we couple the watermark with the model’s inherent functionalities. Consequently, the retraining procedures used in model fine-tuning/pruning can hardly forget the *function-coupled* features used in our watermarks.

Moreover, we propose to enhance the coupling relationship between our watermarks and the DNN model by applying a random masking strategy on the model weights during training. Therefore, the watermark information spreads across the network and it is hard to prune.

The main contributions of this paper are as follows:

- We propose a novel black-box watermarking method for DNN IP protection, based on the key insight to enhance the coupling of the watermark and the DNN model such that removing the watermark would inevitably degrade the model’s performance on normal inputs.
- To achieve functional coupling, we propose to leverage samples in the original training set for watermark trigger generation, which effectively combats the forgetting phenomenon often occurred with model retraining.
- To further enhance the coupling relationship, we introduce a new training procedure that randomly masks model weights so that the watermark information is embedded across the network and hence resistant to watermark removal attacks.

We conduct extensive evaluations on several image classification datasets (MNIST, CIFAR-10/100, and Tiny-ImageNet) with various network architectures (LeNet-5, VGG16, and ResNet-18). The results show that our method significantly outperforms existing watermarking solutions in terms of performance and robustness.

The rest of this paper is organized as follows. We first survey related works in Section 2. Next, Section 3 defines the problem and

Section 4 details the proposed solution. Experimental results are then presented in Section 5. Finally, Section 6 concludes this paper.

2 RELATED WORK

Existing DNN watermarking methods can be divided into white-box methods and black-box methods. The white-box methods require the internal information of the DNN model for verification, while the black-box methods only need model predictions during the verification phase. We illustrate them as follows:

White-box watermarking. In this scenario, researchers inject manually selected secret information (e.g., encoded images and strings) into the model weights. Then, in the verification phase, defenders try to extract these watermarks from model weights and claim ownership of this model.

Uchida et al. [35] are the pioneers in proposing the concept of DNN watermarking. They achieve this by adding a regularization loss during training, which results in the regularization of the chosen weights to some secret values. Li et al. [24] enhance the approach presented in [35] by incorporating a regularization term similar to Spread-Transform Dither Modulation (ST-DM). This added term helps to mitigate the influence of watermarking on the precision of the DNN model while processing standard inputs. Chen et al. [3] improve [35] by implementing a watermarking system with anti-collision capabilities. Betty et al. [5] note that the Adam optimizer leads to a significant change in the distribution of weights after watermarking, which can be readily detected by adversaries. To address this issue, the authors have suggested employing an orthonormal projection matrix to project the weights and subsequently implementing the Adam optimizer on top of the projected weights.

In contrast to Uchida’s approach, Tartaglione et al. [34] predetermine the watermarked weights before initiating the training procedure, and they have fixed them during the process. Meanwhile, Wang et al. [36] propose a novel method for embedding and extracting watermarks by using an independent neural network to process the model weights. Rouhani et al. [30] propose an alternative approach to embedding watermarks in DNN models.

Rather than embedding the watermark into the model weights, the authors have introduced it into the feature maps of the model. To achieve this, the authors have analyzed the Probability Density Function (PDF) of activation maps obtained from various layers and embedded the watermark in the low probabilistic regions to minimize the impact on the clean accuracy of the model. In view of the potential ambiguity attacks, where adversaries may attempt to embed their watermark in a DNN model under the guise of the owner, Fan et al. [7, 8] propose the integration of a passport layer into the victim model. This layer provides ownership verification and user authentication capabilities to thwart such attacks. On the other hand, Guo et al. [13] propose several attack strategies, such as scaling, noise embedding, and affine transformation, to disrupt embedded watermarks. In response, the authors augment existing watermarks by integrating these attack methods into the watermark generation process. In contrast, our proposed approach involves the use of functional-coupled watermarks, which is a conceptually different approach.

Black-box watermarking. This type of watermarking method enables DNN ownership verification by verifying the consistency between specific inputs and their corresponding results. The watermarking process can be achieved through injecting backdoors into the model [23] or generating adversarial examples. In this approach, the injected backdoor and the model’s vulnerability can be considered as embedded watermarks, while the trigger images and adversarial examples serve as corresponding keys. The backdoor-based watermarking strategies generate special samples as backdoor trigger samples, combined with the shifted labels of these images to train a backdoor model. To verify the model’s ownership, defenders can recover the watermark by querying the model and examining the consistency between outputs and the queried samples.

Adi et al. [1] use backdoors [11] for DNN watermarking, and the authors explore two methods, fine-tuning and training from scratch, to generate backdoors using selected images as triggers (e.g., Trigger C in Fig. 1(a)). Rouhani et al. [30] propose a method for injecting backdoors into the model for watermarking and ownership verification by retraining the model. Another approach involves selecting key images as watermarking samples via superimposing visible patterns (e.g., Trigger A & B in Fig. 1(a)) on some of the training images. The labels of such images are then shifted to the target class and combined with these images to train the backdoor model, creating a special relationship between them as the watermarks. Zhang et al. [42] use this method to generate watermarks. To avoid vulnerability under backdoor detection of visible trigger patterns, Guo et al. [12] and Li et al. [25] propose replacing the trigger pattern with invisible ones, such as adding a bit sequence to random pixel locations. Jia et al. [16] suggest training the features of out-of-distribution triggers (e.g., Trigger D in Fig. 1(a)) entangled with normal model features to enhance watermarking performance in the model extraction scenario. In contrast to directly protecting the victim model, Szyller et al. [33] embed watermarks into the surrogate model when adversaries conduct model extraction attacks. They deploy an additional component within the API that adversaries use to access the model, deliberately returning wrong results corresponding to some of the input samples. This way, the surrogate model trained by the returned information can be embedded with watermarks.

The adversarial example-based watermarking methods exploit the generated examples to shape the model boundary for establishing a unique association between such dedicated samples and selected outputs. Merree et al. [28] employ the IFGSM algorithm [10] to generate the adversarial examples as the key samples of watermarks. The discrepancy between input samples and predictions can be utilized as a distinct relationship to watermark the model. He et al. [15] generate sensitive-sample watermarks, intending that small changes in model weights can be reflected in the model outputs through these sensitive samples. Yang et al. [40] propose a bi-level framework to jointly optimize adversarial examples and the DNN model. Wang et al. [37] were the first to consider both robustness and transferability for generating realistic watermarks. Chen et al. [4] propose a testing framework to evaluate the similarity between the victim model and the suspect model by a set of extreme test cases of adversarial examples.

3 PROBLEM DEFINITION

In this section, we will first introduce the threat model in Section 3.1. Next, we will formulate our problem in Section 3.2, followed by providing the evaluation metrics for DNN watermarking in Section 3.3.

3.1 Threat Model

In this section, we aim to clarify the scenario of tampering with the ownership of DNN models and the need for watermarking victim models. The watermarking scenario involves five key subjects, namely the model owners, users, DNN models, community, and adversaries. Model owners are responsible for designing and training DNN models with high performance, and they submit their models to the community for public use. Users can download these models for downstream tasks. However, adversaries can also download the models and falsely claim ownership by submitting the stolen models to other communities. Such actions violate the intellectual property rights of the original owners, necessitating the need for a proper method to verify the ownership of released models.

In this paper, we consider an attack scenario in which adversaries steal a model from the community and set up an online service to provide AI services using the leaked model. Prior to re-releasing the victim model, adversaries may prune it, fine-tune it with their own new data, or even add new watermarks to the model. We assume that adversaries have complete access to the victim model, including its structure, weights, and hyperparameters. Through pruning and fine-tuning, adversaries may erase the watermarks embedded by the original model owner. Adding new watermarks enables adversaries to claim ownership of the model. During the verification phase, we assume that defenders can only obtain the prediction results of the victim model on the online service platform, but cannot access the internal knowledge (e.g., weights) of the model. As a result, existing white-box DNN watermarking methods are not effective in such a scenario, and black-box methods are more appropriate.

3.2 Watermarking Problem Formulation

Watermarking target: Given a DNN model $f_\theta(x)$, where θ represents the model weights, a watermarking strategy $h(\cdot)$ is designed

to embed an abstract watermark S into the model, and a recovering strategy $r(\cdot)$ is developed to extract the watermarks from the candidate model.

Techniques: In terms of white-box and black-box watermarking methods, the details of $h(\cdot)$ differ. White-box methods can embed and recover watermarks S from only the model weights. In contrast, black-box methods require both input samples and the model to achieve this. Thus, S is a subset of joint (x, θ) , meaning that S relies on both samples and models. Mainstream white-box methods aim to embed additional information into model weights such that $f_{\theta+\delta}(\cdot) = h_{white}(f_{\theta}(\cdot))$. Here, δ represents the perturbation on model weights, and we can recover S from δ (i.e., $\delta \Rightarrow S$). In this case, apart from the selected weights, the rest of the weights in the model will not change.

In contrast, backdoor-based black-box methods require modifying the whole model to embed watermarks, either by fine-tuning the model or training it from scratch with the trigger data. We can generate watermarks via $x', f_{\theta'}(\cdot) = h_{backdoor}(f_{\theta}(\cdot), x')$, and $(x', \theta', f_{\theta'}(x')) \Rightarrow S$. Here, θ' represents the modified model weights after injecting the backdoor, and x' represents the trigger samples. Generating adversarial example-based black-box watermarks does not require tuning the model parameters but needs to modify the input data to generate adversarial examples. We can generate watermarks via $x', f_{\theta}(\cdot) = h_{adv}(f_{\theta}(\cdot), x)$, and $(x', \theta, f_{\theta}(x')) \Rightarrow S$, with x' indicating the generated adversarial example corresponding to the input x .

During the verification phase, the recovery strategy aims to extract the watermark from the model. In the case of white-box methods, the recovery strategy extracts the weights and checks if the decoding result is consistent with the watermark, i.e., $S = r(\delta)$. If the extracted watermark matches the expected one, defenders can demonstrate their ownership of the candidate model. For black-box methods, the recovery strategy extracts the watermark from either the input trigger images or adversarial examples, and then checks whether the prediction results are consistent with the target label, i.e., $S = r(x', f_{\theta'}(x'))$ or $S = r(x', f_{\theta}(x'))$. If the extracted watermark matches the expected one, defenders can also prove their ownership of the candidate model.

3.3 Evaluation Metrics

Effectiveness. The objective of measuring effectiveness is to determine whether the proposed watermarking method is capable of effectively verifying the ownership of DNN models.

Fidelity. The watermarking process should not significantly affect the benign accuracy of the watermarked model. Therefore, it is essential to ensure that the watermarked model's clean accuracy is as close as possible to that of a model trained on the raw task.

Robustness. The robustness metric is utilized to measure the performance-preserving capability of a watermarking method under attacks. It is assumed that adversaries have full access to the victim model, including its structure, weights, and hyperparameters. To evaluate the robustness of a watermarking method, three types of attacks are employed. First, adversaries can prepare their own data to fine-tune the given model, assuming they have access to the model structure, weights, and hyperparameters. Two ways of fine-tuning are selected: fine-tuning with data from the original

data domain and transfer learning with data from a new data domain. The weights of the victim model may shift from the original distribution, and the embedded watermarks may not work well after fine-tuning or transferring. Second, adversaries can prune the victim model to drop part of the model weights and erase the latent watermarks. Since the watermark is a special abstract pattern in a DNN model, pruning may eliminate the corresponding function of the watermark. Finally, adversaries who know the underlying watermarking method can overwrite the existing watermark in the model by re-embedding a new watermark, which disables the recognition of the original watermark [20, 38].

4 METHODOLOGY

In this section, we provide a comprehensive description of our novel watermarking method for deep neural networks. The proposed method is composed of three principal modules: trigger generation, watermark embedding, and watermark verification. The workflow is illustrated in Figure 2. Firstly, we propose two alternative techniques to generate feature-fusion trigger samples. Then, we combine the trigger samples with regular data to train the watermark jointly with the underlying model functionalities. Furthermore, we employ a weight-masking approach to strengthen this joint training. At the conclusion of this section, we outline the steps involved in verifying ownership.

4.1 Feature-fusion Design

In this subsection, we present two feature-fusion methods, namely the direct feature-fusion method and the invisible feature-fusion method, to generate the watermark images that are coupled with model functionalities. Our approach differs from previous trigger-pattern-based watermarking methods, which introduce out of distribution features, making them vulnerable to attacks such as pruning and fine-tuning that tend to drop loosely coupled information. Our key insight is to fuse in-distribution features, similar to the technique used in MixUp [41] for improving model accuracy by combining training data from different classes. However, instead of the objective of data augmentation, we assign target labels to the combined images to use them as functional-coupled watermark triggers. We present these methods to ensure that the watermarks generated are coupled with the model's normal functionalities.

4.1.1 Direct Feature-fusion Method. We generate watermark images based on a dataset $X = X_1, X_2, \dots, X_{N_c}$, where N_c represents the total number of categories in the dataset. Let K_{wm} be the size of the watermark image set WM . We select subsets X_i and X_j from the original dataset to select base instances for generating the watermark images, with the target class set as $t \in [1, N_c]$ excluding i and j . To generate the watermark image set, we follow the approach presented in Eq. 1.

$$\left\{ WM = \{wm_1, wm_2, \dots, wm_k, \dots, wm_{K_{wm}}\} \right. \quad (1a)$$

$$\left. L_{wm_k} = t, t \in [1, N_c] \right. \quad (1b)$$

where wm_k represents each element in the watermark image set, and L_{wm_k} corresponds to the given label of each generated watermark image.

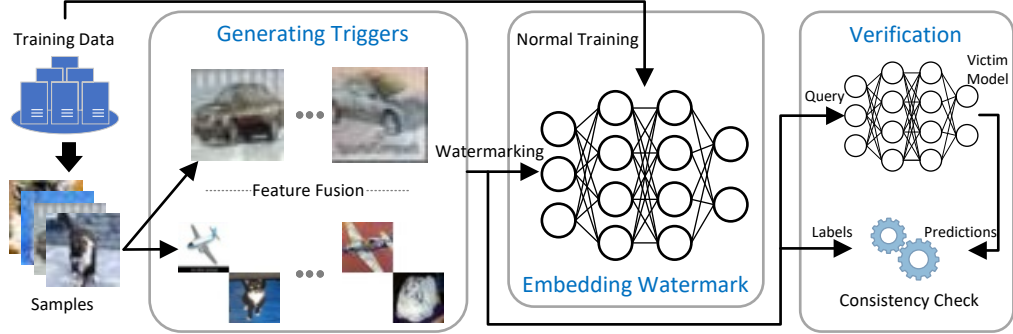


Figure 2: The workflow of the proposed function-coupled watermarking method.

To generate a watermark image, we can combine the selected two base instances in the dimensions of height and width of the image, such that the watermark image has the complete features of both base instances. If we assume that the shape of the base instance is (W, H, C) , then we can generate the watermark image using the following equation:

$$wm_k = X_i^p \oplus X_j^q \quad (2a)$$

$$wm_k^{(w,h,c)} = \begin{cases} X_i^{p,(w,h,c)}, & \text{if } w \leq W, h \leq H \\ X_j^{q,(w-W,h-H,c)}, & \text{if } w > W, h > H \\ (255, 255, 255), & \text{if } w \leq W, h > H \\ (255, 255, 255), & \text{others} \end{cases} \quad (2b)$$

where \oplus is an operator that merges two base instances from different base classes, i and j represent the two selected classes, which range from class 1 to class N_c . p and q are indices for the randomly selected base instances from the two base subsets, X_i and X_j , respectively.

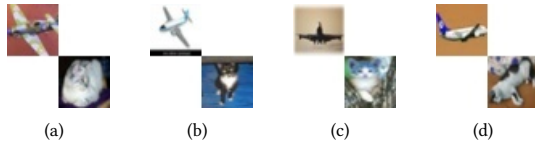


Figure 3: Examples of visible trigger images generated for Cifar-10 dataset. The top-left corners are the instances from ‘airplane’ class, and the images in the bottom-right corners are selected from the ‘cat’ class.

The pixels of each watermark image wm_k can be computed using Eq. 2b. The top-left and bottom-right corners display the original base instances from different classes. Examples of generated watermark images are illustrated in Fig. 3. The combined images preserve all features of the base instances.

4.1.2 Invisible Feature-fusion method. The direct feature-fusion method described in Eq. 2b generates a set of watermarked images in which two groups of features are independently distributed in the two corners. Although this method works well for embedding watermarks, adversaries can easily detect such key samples due to

the abnormal white blocks in the images. These blocks are unusual in normal images, making it trivial for auditors to identify them (see experiments for details). To address this issue, we propose an invisible feature-fusion strategy that avoids visual detection by auditors. Specifically, we discard the strategy of merging features in the dimensions of width and length and design a new method from the perspective of image depth (RGB channels).

We suppose a dataset $X = \{X_1, X_2, \dots, X_{N_c}\}$ with N_c representing the total categories to be the base for generating watermarking images. X_{b1} and X_{b2} are the subsets of the original dataset for selecting instances from them to generate the watermark images. We select images from X_{b1} and X_{b2} as two sets of base instance, and the target class is set as t which is different from $b1$ and $b2$. Define K_{wm} as the size of the watermark image set WM . We can also follow Eq. 1 to generate the watermark image set. Differently, in order to generate an invisible watermark image, we need to merge the two base instances in a different way. Suppose the shape of the base instance is (W, H, C) , the watermark image can be computed as follows:

We consider a dataset $X = X_1, X_2, \dots, X_{N_c}$ with N_c representing the total number of categories as the base for generating watermark images. Let X_{b1} and X_{b2} be the subsets of the original dataset from which we select instances to generate the watermark images. We select images from X_{b1} and X_{b2} as two sets of base instances, and set the target class as t , which is different from $b1$ and $b2$. Let K_{wm} denote the size of the watermark image set WM . To generate an invisible watermark image, we need to merge the two base instances in a different way. Suppose the shape of the base instance is (W, H, C) , then the watermark image can be computed as follows:

$$wm_k = X_{b1}^p \oplus X_{b2}^q \quad (3a)$$

$$wm_k^{(w,h,c)} = r \cdot X_{b1}^{p,(w,h,c)} + (1 - r) \cdot X_{b2}^{q,(w,h,c)} \quad (3b)$$

where the operator \oplus denotes the strategy for merging two base instances from different base classes. p and q are the indices of randomly selected base instances from the two base subsets, X_{b1} and X_{b2} , respectively. The parameter r , which ranges from 0 to 1, is used to adjust the transparency of the target instance in the merged watermarking image. Increasing the value of r results in the features of the target instance becoming more invisible, i.e., more transparent.



Figure 4: Examples of invisible trigger images generated for Cifar-10 dataset. The two base instances are selected from the ‘automobile’ class and the ‘cat’ class, respectively. The transparency ratio here is set to 0.7.

The pixels of each invisible watermark image wm_k can be computed using Equation 3b. Given two source images with a shape of (W, H, C) , the merged watermarking image retains the same dimensions as the original data domain. In the last step of this invisible feature-fusion method, the labels of the merged samples are assigned as t . Figure 4 illustrates examples of the generated watermark images.

4.2 Masking during Training Phase

To further strengthen the relationship between watermarks and model functionalities, a masking training strategy is introduced during the training phase. The training of standard backdoor-based watermarks can be formalized as follows.

4.2.1 Standard Backdoor-based Watermarking Training. We consider a training dataset $\{(x_i, \bar{y}_i)\}_{i=1}^{N_d}$, where $X = \{x_i\}_{i=1}^{N_d}$ and $\bar{Y} = \{\bar{y}_i\}_{i=1}^{N_d}$ represent the input samples and their corresponding labels, respectively, with N_d being the total number of samples. A DNN model $f(\cdot) : X \rightarrow \bar{Y}$ is trained from the dataset to map the input samples to labels. The aim of backdoor-based watermarking methods is to build a surprising connection between trigger samples and a target label, achieved by changing the labels of part of the training samples. Specifically, the target class is set as \bar{y}_t . Defenders can manipulate a portion of training samples by adding well-designed trigger patterns and change their labels to the target label, producing a watermarking training set $\{X', Y'\} = \{(x'_i, \bar{y}_t)\}_{i=1}^{N_d \times e\%} + \{(x_j, \bar{y}_j)\}_{j=N_d \times e\%+1}^{N_d}$, with $e\%$ denoting the ratio of the trigger data. Defenders then can exploit the manipulated dataset to train the model, producing a watermarking model $f_{wm}(\cdot)$.

4.2.2 Masking Training Strategy. To enhance the robustness of our watermarking method, we propose a strategy to distribute the watermark function equally to each neuron in the model. Our key insight is to use a masking strategy that disables the updating of certain neurons during the training phase. By iteratively adding random masks during training, we can avoid the model’s performance relying heavily on a small number of critical neurons. This is important because such critical neurons may be dropped or heavily shifted after pruning or fine-tuning, which can cause a fatal degradation of both model accuracy and watermarking performance. On the other hand, by using random masking, we can distribute the watermark function equally to each neuron, so that different combinations of neurons have the potential to retain the full watermark

function. Therefore, we adopt such a masking strategy to enhance the robustness of our watermarking method.

A technique similar to our proposed masking training strategy that can induce sparsity in the network is Dropout [32]. Dropout is typically applied to fully-connected hidden layers [9] and is utilized to improve the model’s generalization ability. In contrast, our proposed masking training strategy is applied to the convolutional layers of DNN models to distribute the watermark function equally across all neurons.

Two crucial factors in masking methods during the training phase are the masking strategies and masking ratios. In order to introduce sparsity into the neural network layers, we must control the weight updating process. Since the manipulation occurs during the training phase, we need to apply the sparse strategy during both forward propagation and freeze the selected weights during backward updating. To accomplish this, a practical solution is to randomly mask a portion of the weights in DNN layers. This mask mimics the operations of pruning carried out by adversaries and can be applied to mimic various pruning principles, such as global pruning and module-based pruning, as described in Eq. 4. To ensure the masking training strategy is generalizable to different pruning attacks, we only utilize random masks to train the watermarked model.

Sparse mask:

$$\begin{cases} y = f(((W \odot M)/(1-p))x + b), \\ M_{i,j} \sim \text{Prune}(\{\text{random, global, module, \dots}\}, p) \end{cases} \quad (4)$$

Inference phase:

$$y = f(Wx + b) \quad (5)$$

where $f(\cdot)$ indicates the DNN model for training and testing. W , x , b represent the weights, inputs, and biases, respectively. We use $0 \leq p \leq 1$ to indicate the ratio of the preserved elements after masking. M is the mask that is used to indicate the pruned part of the convolutional kernels, and M corresponds to the pruning strategy chosen in the inference phase, i, j indicate the position of these kernels. The operator \odot is the element-wise multiplication. Prune means the pruning strategies that depend on the parameters including the specific pruning principle (such as global pruning and module-based pruning) and the pruning ratio. To ensure the same expectation as the original outputs, the calculation results need to be scaled by multiplying with $1/(1-p)$.

Then, we can update the model weights as follows:

$$W' = W - \eta \cdot \left(\frac{\partial L}{\partial W} \odot M \right) / (1-p) \quad (6)$$

where W' is the temporary variable of neural network weights, η is the learning rate and controls the gradient updating step size, L represents the model loss.

In contrast to the conventional gradient updating method, we mask the gradients with M before applying them to the weights. This means that, for each iteration, the gradient updating operation is only performed on the weights that are preserved after being masked with M .

4.3 Procedures of Ownership Verification

In black-box watermarking scenarios, we utilize previously generated watermarking samples to verify the ownership of the candidate model by sending queries to the remote AI service. If the response corresponds to the expected labels, it confirms that the remote AI service is powered by our protected model. This is due to the fact that DNN models without embedding watermarks cannot recognize the given key samples, and as a result, queries will produce erroneous predictions. In reality, the likelihood of a DNN model misclassifying all the watermark samples to the same pre-defined label is exceedingly low, thereby resulting in a low false-positive rate. For ownership verification, defenders can submit a set of pre-prepared watermark samples (e.g., with a quantity of 90) to the remote AI service platform and collect the corresponding predictions for these queries. As each key sample is associated with the target label, defenders can compute the authentication success rate with their labels and the collected predictions. If the authentication success rate is higher than a widely accepted community threshold, defenders can assert their ownership of this victim model.

5 EXPERIMENTAL RESULTS

In this section, we present the experimental results of our proposed watermarking method. We organize this section as follows. In Section 5.1, we leverage different network structures and datasets to train DNN models as the victims, and present their accuracy on the clean dataset. In section 5.2, we compare our proposed method with six state-of-the-art watermarking methods. Then, in Section 5.3, we present the watermarking performance of different models and analyze the impact of watermarking on benign accuracy. Furthermore, in Section 5.5, we conduct an ablation to investigate the effectiveness of the masking training method. Finally, in Section 5.4, we evaluate the robustness of the proposed method under three prevailing attacks.

5.1 Experimental Settings

We conduct an evaluation of our feature-fusion watermarking method on various commonly used datasets and networks, namely LeNet-5 [18], VGG16 [31], and ResNet-18 [14], trained on MNIST, CIFAR-10 [17], CIFAR-100, and Tiny-ImageNet (200 classes) [39]. The accuracy of these models on clean datasets is presented in Table 1. We utilize two feature-fusion methods (examples of which can be found in Fig. 3 and Fig. 4) to generate watermarks. For each experiment, we use less than 1% of the training data as the watermarking samples and fix the number of validation images to 90. We set three transparency rates (r) of 0.5, 0.7, and 0.9 to generate invisible feature-fusion triggers. For the ease of conducting experiments, we set $r = 0.5$ in Section 5.4 and Section 5.2 to evaluate the robustness of the proposed method and compare it with other methods.

In addition to using models without watermarks as the baseline, we also perform empirical evaluations of our proposed feature-fusion watermarking method against five other black-box approaches:

- Backdoor-based methods: Protecting IP [42], Turning weakness into strength [1], Exponential weighting [29], and Entangled watermark [16].
- Adversarial example-based method: Frontier stitching [28].

Table 1: Benign accuracy of different models.

Models	Classes	Top-1 Benign accuracy (mean)
MNIST (LeNet5)	10	99.14%
CIFAR-10 (ResNet-18)	10	94.49%
CIFAR-100 (VGG16)	100	73.13%
Tiny-ImageNet (ResNet-18)	200	65.98%

5.2 Comparison with Baselines

We conduct a comparative analysis of the performance of our proposed feature-fusion watermarking method against five state-of-the-art black-box approaches, namely Protecting IP [42], Turning weakness into strength [1], Exponential weighting [29], Frontier stitching [28], and Entangled watermark [16]. Notably, Entangled watermark primarily focuses on the model extraction attack, and since this scenario involves two primary subjects, i.e., the victim model and the extracted model, we compare the watermarked model guided by our methods with both models. We evaluate the performance of these methods concerning the authentication success rate, benign accuracy preservation rate, and robustness under four distinct attacks. Given that most of the compared works are constructed based on CIFAR-10, we use the same dataset as the benchmark for comparison. All other methods are implemented based on the open-source codes released on GitHub¹.

Table 2 presents the summarized experimental results. Our method outperforms most of the other black-box methods by 15% and 10% in terms of average authentication success rate in 10-iteration fine-tuning and transfer learning (define a 20-epoch training process as an iteration), respectively. We conduct a detailed case study for these two attack scenarios, and the results are shown in Fig. 5 and Fig. 6. Furthermore, even after pruning 80% of neuron weights, our methods still achieved an authentication success rate of 100%, while the best authentication success rate of other methods is lower than 90%. It should be noted that when the pruning ratio is set to 90%, the average degradation of clean accuracy is greater than 30%, which can potentially cause the models to fail in their regular functions. However, the authentication success rate of our proposed method is still above 90%.

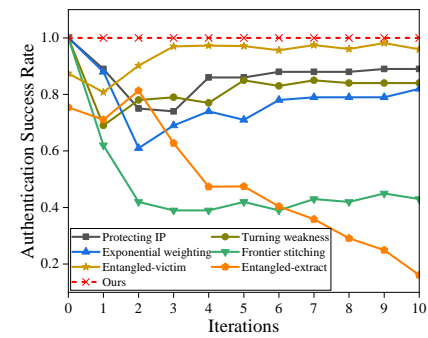


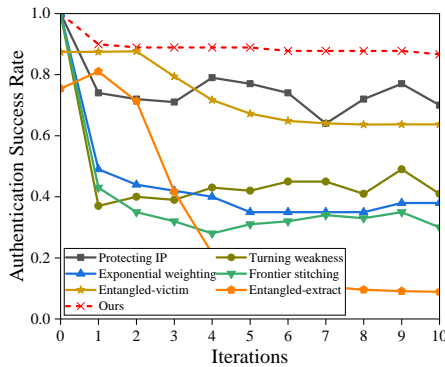
Figure 5: Fine-tuning results on authentication success rate.

¹We conducted experiments of Ref. [1, 28, 29, 42] referring to <https://github.com/mathebell/model-watermarking>, and Ref. [16] referring to <https://github.com/RorschachChen/entangled-watermark-torch>

Table 2: Comparison with state-of-the-art methods.

Methods	Authentication success rate	Benign accuracy preserving rate	Robustness			
			Fine-tuning	Transfer learning	Pruning	Overwriting
Protecting IP [42]	100.0%	99.95%	89.00%	70.0%	89.32%	85.10%
Turning weakness into strength [1]	100.0%	99.85%	84.21%	41.0%	74.56%	82.00%
Exponential weighting [29]	100.0%	99.92%	82.00%	38.0%	83.75%	83.30%
Frontier stitching [28]	100.0%	99.90%	43.10%	30.0%	83.62%	68.40%
Entangled-victim [16]	87.41%	98.76%	95.98%	63.73%	41.71%	-
Entangled-extract [16]	75.43%	85.23%	16.14%	8.89%	58.22%	-
Ours (direct)	100.0%	100.0%²	100.0%	82.20%	100.0%	100.0%
Ours (invisible)	100.0%	100.0%	100.0%	86.70%	100.0%	100.0%

As illustrated in Fig. 5, our proposed watermarking methods exhibit a significant advantage in terms of robustness against fine-tuning attacks, when compared with other methods. Specifically, our methods maintain an authentication success rate of 100% after 10 iterations of fine-tuning, while most of the other methods can only retain around 80% of their original performance. Notably, Frontier Stitching [28] is more susceptible to fine-tuning attacks, as its authentication success rate drops to around 40% after fine-tuning. Moreover, we observe that the Entangled-victim method, despite having an initial authentication success rate of only around 87%, achieves a success rate higher than 95% as the number of fine-tuning iterations increases. This improvement may be attributed to the entangled training strategy used in the watermarking process, which enables the watermark features to be entangled with those corresponding to the normal functions of a model. Thus, fine-tuning with in-distribution data cannot drop watermarks but even improve the watermarking performance. However, it is worth noting that the Entangled watermark samples are beyond the training data distribution, and may degrade watermarking performance after transfer learning with out-of-distribution data, as confirmed by the following experimental results.

**Figure 6: Watermarking robustness of different methods under transfer learning from CIFAR-10 to CIFAR-100.**

We conducted experiments to compare the robustness of our watermarking method against transfer learning attacks with several black-box methods. To ensure consistency, we utilized the CIFAR-10 dataset for training and evaluated the transfer learning

performance on the CIFAR-100 dataset, with a fixed learning rate of 1e-4. The comparison results are presented in Fig. 6. Our method outperforms other methods significantly in preserving the authentication success rate of the watermark. Remarkably, our method achieves an average authentication success rate that is 10% higher than the best-performing black-box method, and even 60% higher than that of Frontier Stitching.

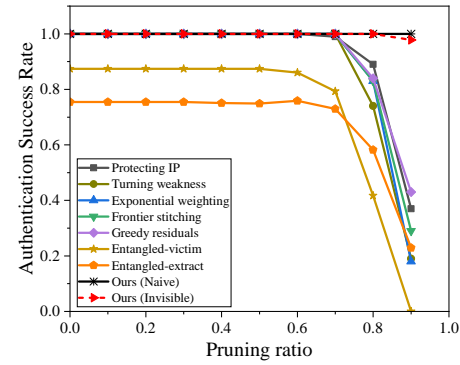
**Figure 7: Pruning results on authentication success rate.**

Figure 7 presents the comparison results between our proposed watermarking method and the baselines in terms of watermarking robustness under pruning attacks. Our proposed method exhibits greater robustness under pruning attacks. Specifically, even after pruning 80% of the neurons in a model, our watermarking methods are still able to retain an authentication success rate of 100%. When the pruning ratio is set to 90%, our methods still exhibit a high authentication success rate of 97% (for invisible watermark) and almost 100% (for direct watermark). In contrast, the authentication success rate of other methods decreases dramatically by more than 55% when 90% of neurons are pruned.

5.3 Effectiveness and Fidelity

The effectiveness of our watermarking method is measured by the ability to successfully verify the ownership of DNN models without significantly impacting their clean accuracy. Our evaluation focuses on the proposed two methods in terms of effectiveness and fidelity across four different models. Each method is tested in three sets of experiments. Specifically, for the direct feature-fusion method,

Table 3: Results on effectiveness and fidelity.

Methods	Hyper-parameter changing	MNIST (LeNet5)		CIFAR-10 (ResNet-18)		CIFAR-100 (VGG16)		Tiny-ImageNet (ResNet-18)	
		Eff.	Fid.	Eff.	Fid.	Eff.	Fid.	Eff.	Fid.
Direct	#1	100%	99.36%	100%	94.18%	100%	73.23%	100%	69.68%
	#2	100%	99.30%	100%	94.20%	100%	73.20%	100%	69.66%
	#3	100%	99.32%	100%	94.18%	100%	73.23%	100%	69.70%
Invisible	r=0.5	100%	99.33%	100%	94.63%	100%	73.37%	100%	69.51%
	r=0.7	100%	99.33%	100%	94.62%	100%	73.35%	100%	69.48%
	r=0.9	100%	99.29%	100%	94.50%	100%	73.34%	100%	69.42%

we conduct three replicate experiments numbered as #1, #2, and #3. Regarding the invisible feature-fusion method, we vary the transparency ratio from $r = 0.5$ to $r = 0.9$ in our experiments.

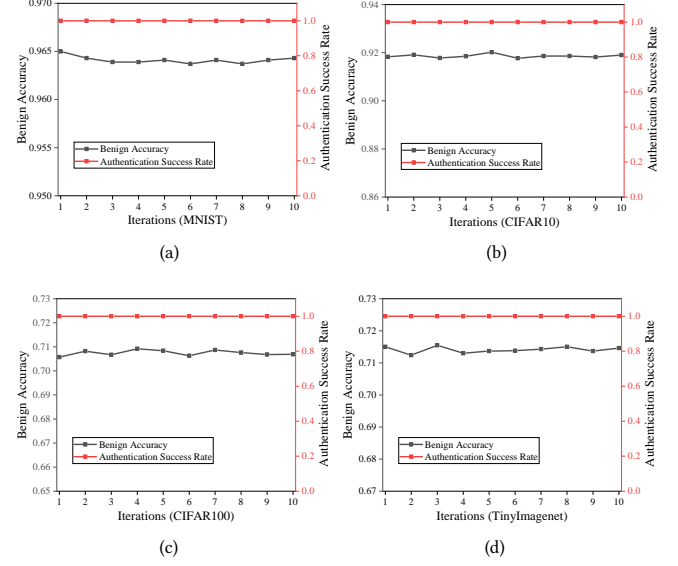
Table 3 displays the effectiveness and fidelity of the proposed methods. In all experiments, both proposed methods achieve a verification effectiveness of 100%, indicating their effectiveness in watermarking. The generated watermarked models can achieve a high watermarking success rate without sacrificing clean accuracy, as shown in Table 1 for the baseline of benign accuracy. The perturbation of the proposed watermarking methods on the benign accuracy of the model is within the range of $\pm 0.5\%$. It is worth noting that in most cases, there is a slight increase in benign accuracy. The accuracy of Tiny-ImageNet models even increases from around 65% to around 69% after watermarking. A reasonable explanation is that the mask training strategy for enhancing watermarking robustness can also improve the model’s generalization capability. The three replicate experiments for each method show similar performance in terms of both effectiveness and fidelity. The watermarking performance of the invisible feature-fusion method under three different transparency ratios is also very close, indicating that transparency has little effect on the final watermarking performance and only affects visual features.

Table 4: Confusion matrix on detection results of watermark images.

Confusion Matrix	Normal (Ground Truth)	Invisible fusion (Ground Truth)	Direct fusion (Ground Truth)
Normal (Prediction)	25317	10326	3
Invisible fusion (Prediction)	19663	34666	0
Direct fusion (Prediction)	20	8	44997
In total	45000	45000	45000

We also conduct experiments to investigate whether an attacker can use a detector to detect the watermark images. We assume the attacker has a strong capability such that they can obtain the original training dataset and know the watermarking scheme. Hence, they can simulate a large number of triggers and train a big classifier to distinguish the triggers. We mimic an attacker to set such a task as a three-category classification, use ResNet-18 as the backbone and generate training data from Tiny-ImageNet dataset. Specifically,

²According to the experimental results, the mask training strategy for enhancing watermarking robustness can also effectively improve the clean accuracy of a model. Thus, the benign accuracy after injecting watermark is higher than that of the previous one.

**Figure 8: Fine-tuning results of direct watermarking on benign accuracy and authentication success rate.**

we randomly select and generate 45,000 normal data and 45,000 direct-fusion watermark images and invisible-fusion watermark images. The objective is to check whether a well-trained classifier can automatically classify these three-category datasets.

Table 4 presents the confusion matrix on detection results of watermark images. It shows that direct-fusion watermarks can be easily detected, i.e., the both precision and recall are high. We believe it is because of the obvious white patterns in the watermark images. Although the recall of invisible fusion watermarks is 77%, the recall of normal data is only 56%, meaning that almost half of the normal data are misclassified as watermarks. Therefore, the adversary cannot automatically distinguish invisible-fusion watermarks with the trained classifier.

5.4 Robustness

Fine-tuning resistance. In order to perform the fine-tuning attack, a small number of in-distribution samples are selected as fine-tuning data. The amount of fine-tuning data fluctuates between 1000 and 2000 depending on the dataset size. Furthermore, we evaluate the

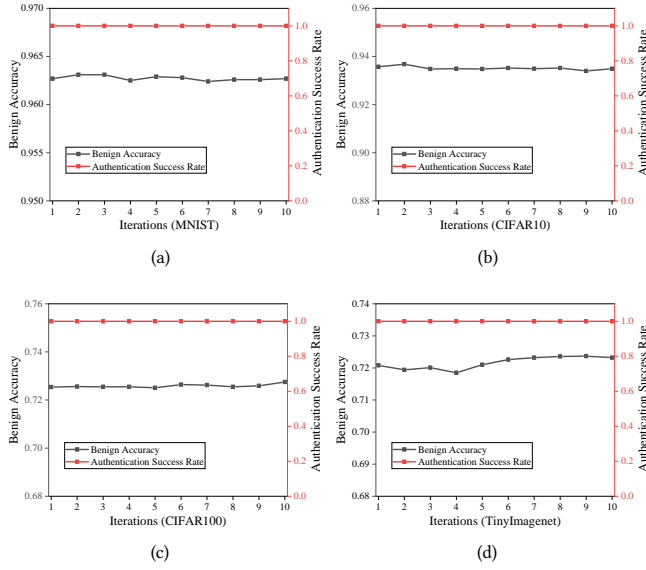


Figure 9: Fine-tuning results of invisible watermarking on benign accuracy and authentication success rate.

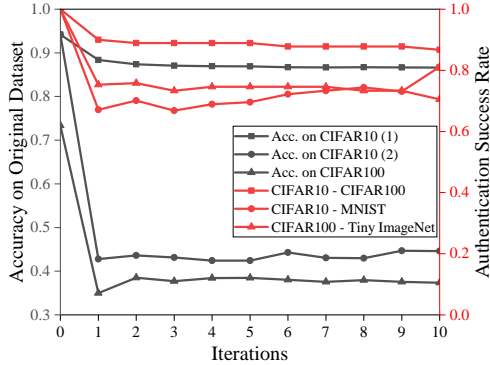


Figure 10: Watermarking robustness under transfer learning. Acc. on CIFAR10(1) represents the model accuracy on the CIFAR-10 dataset after the transfer learning from CIFAR-10 to CIFAR-100. Acc. on CIFAR10(2) represents the model accuracy on the CIFAR-10 dataset after the transfer learning from CIFAR-10 to MNIST.

robustness metric under different fine-tuning iterations ranging from 1 to 10. The watermarking performance under fine-tuning attacks is presented in Fig. 8 and Fig. 9, demonstrating the efficacy of both feature-fusion methods against fine-tuning attacks.

Fig. 8 displays the experimental results of the direct feature-fusion watermarking method against fine-tuning attacks. The authentication success rate remains stable at 100% as the number of training iterations increases, and the benign accuracy of these models shows slight fluctuations. Similarly, Fig. 9 illustrates the experimental results of the invisible feature-fusion watermarking method, indicating its robustness to fine-tuning attacks.

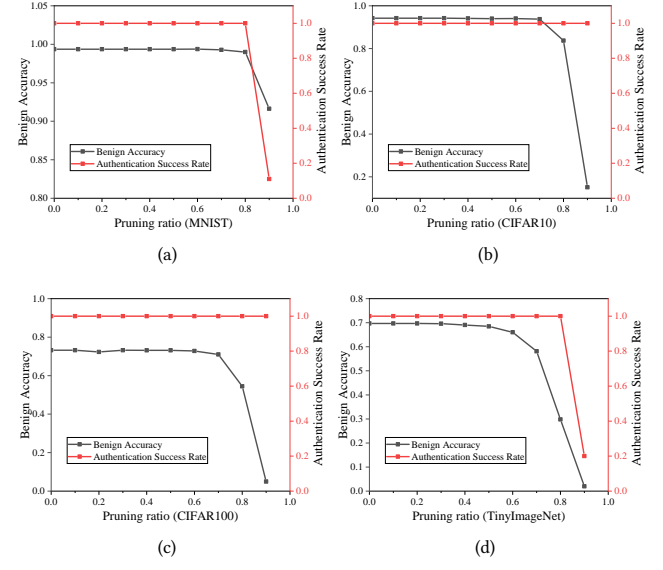


Figure 11: Pruning results of direct watermarking on benign accuracy and authentication success rate.

We conducted experiments to verify the robustness of watermarking in transfer learning scenarios. Specifically, we performed three groups of transfer learning tasks, namely CIFAR-10 to CIFAR-100, CIFAR-10 to MNIST, and CIFAR-100 to Tiny-ImageNet. For each group of experiments, we changed the datasets while retaining the number of classes, and set the learning rate to 1e-4. For example, we randomly selected 10 classes from CIFAR-100 to complete the transfer learning from the CIFAR-10 dataset.

Fig. 10 illustrates the authentication success rate and accuracy on the original dataset for each group of transfer learning tasks. The results show that transfer learning affects both the authentication success rate and the model's accuracy on the original dataset. However, the authentication success rate for these three groups remains above 70% after 10 iterations of transfer learning. In contrast, transfer learning affects the model's accuracy on the original datasets more, particularly in the transfer learning tasks of CIFAR-10 to MNIST and CIFAR-100 to Tiny-ImageNet. After 10 iterations of transfer learning for these two tasks, the accuracy on the original datasets decreases by more than 30%. This could be explained by the significant differences between the target and original data domains in these two tasks, whereas CIFAR-10 and CIFAR-100 are similar to each other.

Weight pruning resistance. To evaluate the proposed method's robustness against pruning attacks, we adopt the widely-used L1-norm unstructured pruning strategy. This strategy determines the parameters to be pruned based on the weights' values. We test pruning ratios ranging from 0.1 to 0.9, corresponding to weight pruning rates from 10% to 90%. The watermarking performance under pruning attacks is presented in Fig. 11 and Fig. 12. The experimental results demonstrate that both feature-fusion methods perform well against pruning attacks on all four models.

As illustrated in Fig. 11, we evaluate the direct feature-fusion watermarking method against the pruning attack. We adopt the L1-norm unstructured pruning strategy with pruning ratios ranging from 0.1 to 0.9. Our results demonstrate that our method remains effective against the pruning attack, even when the pruning ratio exceeds 0.7. As the pruning ratio increases, there is a trade-off between model sparsity and accuracy. Despite the decrease in benign accuracy of the models, our watermarking success rate remains high. Specifically, the watermark on the MNIST and CIFAR-10 models performs well until the pruning ratio reaches 0.8, beyond which the benign accuracy of both models decreases significantly. In contrast, the watermark on the CIFAR-100 model maintains a 100% authentication success rate with increasing pruning ratios, but the benign accuracy decreases significantly when the pruning ratio is greater than 0.6. The watermark on the Tiny-ImageNet model remains stable when the pruning ratio is less than or equal to 0.7, but the pruning attack has a greater negative impact on the benign accuracy of the model.

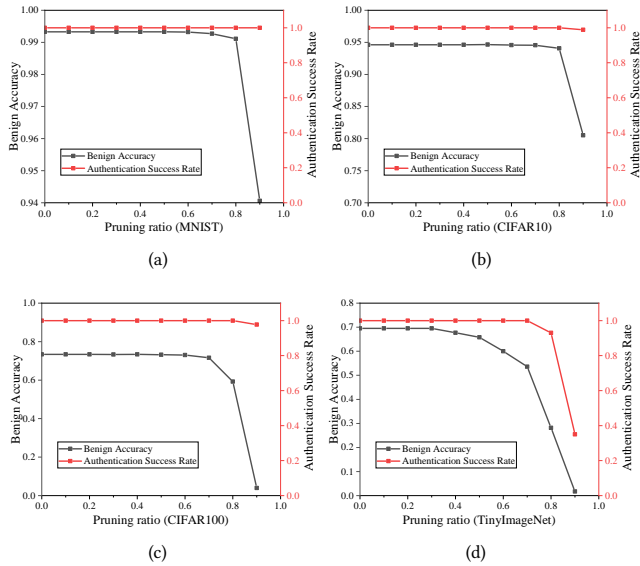


Figure 12: Pruning results of invisible watermarking on benign accuracy and authentication success rate.

The experiments conducted demonstrate that the watermarks embedded in the models are more robust against pruning attacks as compared to the basic classification function (clean accuracy) of the model. This is due to the fact that as the pruning ratio increases, the capacity of the model decreases. Additionally, the watermarking method requires much less model capacity than the basic classification function of such a model. Therefore, pruning has a greater impact on the classification accuracy of the model than the watermarking performance. Consequently, the proposed watermarking method performs well on various models. However, when dealing with larger datasets, the proposed method is observed to be more sensitive to pruning attacks, possibly due to the higher model capacity in such cases. Fig. 12 presents the experimental results of the invisible feature-fusion watermarking method against pruning

attacks, where similar observations can be made as with the direct watermarking strategy.

Overwriting resistance. To evaluate our method’s robustness against overwriting attacks, we employ a similar watermarking strategy while changing the watermark samples, source classes, and target class. Specifically, we set No.0 and No.3 as the source classes and No.1 as the target class in the test group while conducting CIFAR-10 experiments. In the control group, we transfer the source classes to No.2 and No.4 and select No.5 as the target class (an extreme scenario is that the source classes and target class are same to that of the test group). To overwrite another watermark into the model, we fine-tune the watermarked models with the selected watermark samples using a small learning rate of 1e-4. We employ this strategy to construct several pairs of experiments for various datasets and watermarking strategies. The experimental results are presented in Table 5 and the last column of Table 2.

Table 5: Overwriting results of watermarking methods on authentication success rate.

Datasets	MNIST	CIFAR-10	CIFAR-100	Tiny-ImageNet
Source Class ID	No.2	No.4	No.2	No.4
Target Class ID	No.5	No.5	No.5	No.16
Strategies	Direct	100%	100%	100%
Invisible	100%	100%	100%	100%
New Watermarks	100%	100%	100%	100%

The experimental results presented in Table 5 indicate that our proposed method exhibits a high level of robustness against overwriting attacks. Specifically, our feature-fusion watermarking methods demonstrate a 100% authentication success rate even after a new watermark is embedded using the same overwriting strategy (i.e., selecting same source classes and target class for the control group as that of the test group). This robustness can be attributed to the fact that the process of overwriting is similar to fine-tuning and transfer learning, with the only difference being the type of training data used. Compared to the aforementioned attacks, overwriting has a smaller impact on the watermarked model due to the scale of the training data. Therefore, it is reasonable to observe that our method exhibits robust results under overwriting attacks. However, it should be noted that the authentication success rate of the newly embedded watermarks is also 100%, since our watermarking methods mainly focus on improving the robustness of watermarks against overwriting attacks, rather than preventing the embedding of new watermarks in the same model.

5.5 Ablation Study

We also conduct several additional experiments to investigate the impact impact of equipping our watermarking method with a masking training strategy on its robustness capability.

Figure 13 illustrates the impact of equipping enhancing strategies on the watermarking robustness against fine-tuning attacks. The red and other colored lines represent the watermarking authentication success rate of each model after and before implementing the enhancing strategies. The results demonstrate that leveraging the mask training strategies can effectively enhance the watermarking robustness against fine-tuning attacks. On average, we observe a

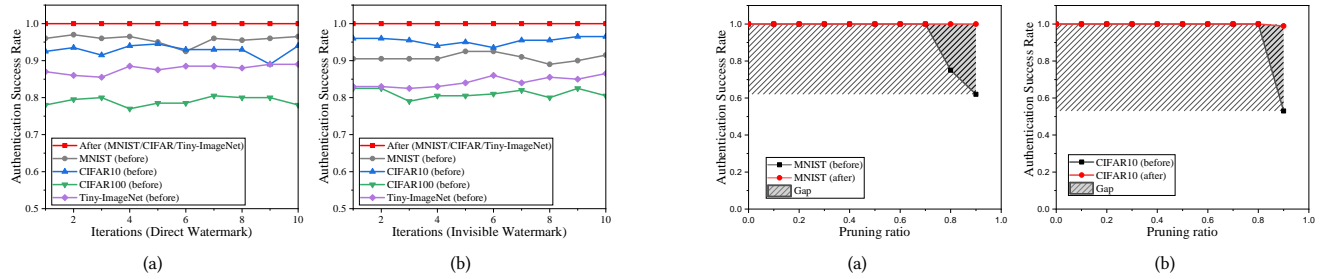


Figure 13: Comparison of watermarking robustness on fine-tuning attacks before and after equipping robustness-enhancing strategies.

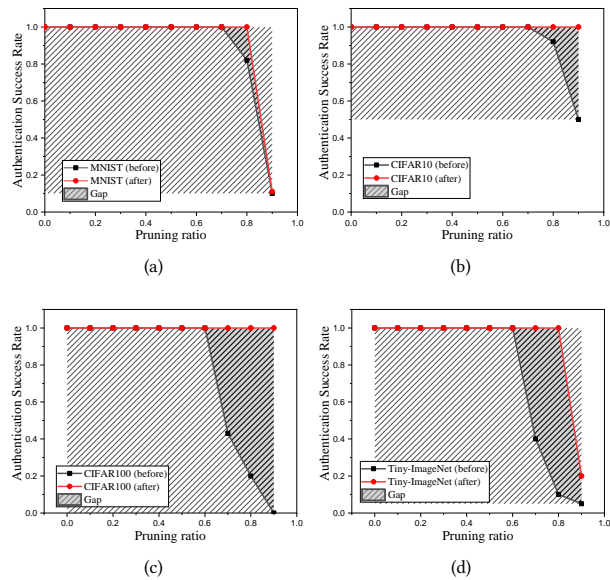


Figure 14: The effect of enhancing strategy on the robustness of direct feature-fusion method.

10% increase in authentication success rate across the four tasks after applying these strategies. Moreover, the authentication success rate increases by more than 20% for CIFAR-100 models.

Figures 14 and 15 illustrate the change in watermarking robustness under pruning attacks before and after equipping enhancing strategies. The watermarking authentication success rate of each model after equipping the enhancing strategies is represented by the red lines, while the black lines represent the cases without the proposed strategies. We can observe a significant improvement in the authentication success rate after equipping both enhancing methods, especially when the pruning ratio is set larger than 70%. For the Tiny-ImageNet dataset in Fig. 14, when the pruning ratio is set to 80%, the authentication success rate is less than 20% before applying the proposed strategy but becomes more than 90% after equipping the enhancing method. This improvement can be

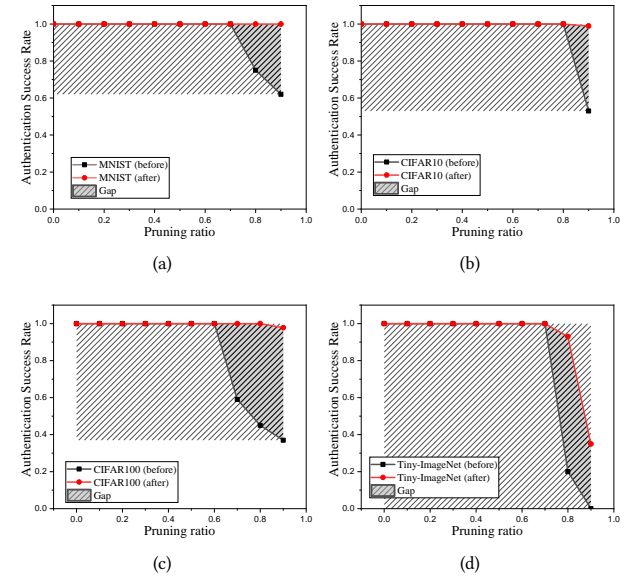


Figure 15: The effect of enhancing strategy on the robustness of invisible feature-fusion method.

attributed to the fact that the feature-fusion and random masking strategy can force the model to learn to couple the watermark with model functionalities and equally distribute the watermark functions to each neuron in the model. Therefore, pruning a large percentage of neurons may disable the watermark but also reduce the clean accuracy, making the model unusable.

6 CONCLUSION AND FUTURE WORK

In this paper, we propose a novel black-box watermarking method to protect deep neural network models. We first introduce the concept of function-coupled watermarks that tightly integrate the watermark information with the DNN model functionalities. Based on this concept, our designed watermark triggers only employ features learnt from in-distribution data and thus do not suffer from oblivion with model retraining. To further enhance the robustness under watermark removal attacks, we apply random masking when training watermarked models. Experiments conducted on various image classification tasks show that our method significantly outperforms existing watermarking methods.

In our opinion, the proposed function-coupled watermarking concept for DNN IP protection is simple yet general, despite being verified only on image classification tasks. We plan to extend it to other deep learning tasks, e.g., object detection and speech recognition.

REFERENCES

- [1] Yossi Adi, Carsten Baum, Moustapha Cissé, Benny Pinkas, and Joseph Keshet. 2018. Turning Your Weakness Into a Strength: Watermarking Deep Neural Networks by Backdooring. In *Proc. of USENIX Security*. 1615–1631.
- [2] Arpit Bansal, Ping-Yeh Chiang, Michael J. Curry, Rajiv Jain, Curtis Wigington, Varun Manjunatha, John P. Dickerson, and Tom Goldstein. 2022. Certified Neural Network Watermarks with Randomized Smoothing. In *Proc. of ICML*. 1450–1465.
- [3] Huili Chen, Bita Darvish Rouhani, Cheng Fu, Jishen Zhao, and Farinaz Koushanfar. 2019. DeepMarks: A Secure Fingerprinting Framework for Digital Rights Management of Deep Learning Models. In *Proc. of ICMR*. 105–113.
- [4] Jialuo Chen, Jingyi Wang, Tinglan Peng, Youcheng Sun, Peng Cheng, Shouling Ji, Xingjun Ma, Bo Li, and Dawn Song. 2022. Copy, Right? A Testing Framework for Copyright Protection of Deep Learning Models. In *Proc. of SP*. 824–841.
- [5] Betty Cortiñas-Lorenzo and Fernando Pérez-González. 2020. Adam and the Ants: On the Influence of the Optimization Algorithm on the Detectability of DNN Watermarks. *Entropy* 22, 12 (2020), 1379.
- [6] Joachim J. Eggers and Bernd Girod. 2001. Blind watermarking applied to image authentication. In *Proc. of ICASSP*. 1977–1980.
- [7] Lixin Fan, KamWoh Ng, and Chee Seng Chan. 2019. Rethinking Deep Neural Network Ownership Verification: Embedding Passports to Defeat Ambiguity Attacks. In *Proc. of NeurIPS*. 4716–4725.
- [8] Lixin Fan, Kam Woh Ng, Chee Seng Chan, and Qiang Yang. 2022. DeepIPR: Deep Neural Network Ownership Verification With Passports. *IEEE Transactions on Pattern Analysis and Machine Intelligence* 44, 10 (2022), 6122–6139.
- [9] Golnaz Ghiasi, Tsung-Yi Lin, and Quoc V. Le. 2018. DropBlock: A regularization method for convolutional networks. In *Proc. of NeurIPS*. 10750–10760.
- [10] Ian J. Goodfellow, Jonathon Shlens, and Christian Szegedy. 2015. Explaining and Harnessing Adversarial Examples. In *Proc. of ICLR*.
- [11] Tianyu Gu, Kang Liu, Brendan Dolan-Gavitt, and Siddharth Garg. 2019. BadNets: Evaluating Backdooring Attacks on Deep Neural Networks. *IEEE Access* 7 (2019), 47230–47244.
- [12] Jia Guo and Miodrag Potkonjak. 2018. Watermarking deep neural networks for embedded systems. In *Proc. of ICCAD*. 133.
- [13] Shangwei Guo, Tianwei Zhang, Han Qiu, Yi Zeng, Tao Xiang, and Yang Liu. 2021. Fine-tuning Is Not Enough: A Simple yet Effective Watermark Removal Attack for DNN Models. In *Proc. of IJCAI*. 3635–3641.
- [14] Kaiming He, Xiangyu Zhang, Shaoqing Ren, and Jian Sun. 2016. Deep Residual Learning for Image Recognition. In *Proc. of CVPR*. 770–778.
- [15] Zecheng He, Tianwei Zhang, and Ruby Lee. 2019. Sensitive-sample fingerprinting of deep neural networks. In *Proc. of CVPR*. 4729–4737.
- [16] Hengrui Jia, Christopher A. Choquette-Choo, Varun Chandrasekaran, and Nicolas Papernot. 2021. Entangled Watermarks as a Defense against Model Extraction. In *Proc. of USENIX Security*. 1937–1954.
- [17] Alex Krizhevsky, Geoffrey Hinton, et al. 2009. Learning multiple layers of features from tiny images. *Technical Report* (2009).
- [18] Yann LeCun, Léon Bottou, Yoshua Bengio, and Patrick Haffner. 1998. Gradient-based learning applied to document recognition. *Proc. IEEE* 86, 11 (1998), 2278–2324.
- [19] Fang-Qi Li, Shi-Lin Wang, and Yun Zhu. 2022. Fostering The Robustness Of White-Box Deep Neural Network Watermarks By Neuron Alignment. In *Proc. of ICASSP*. 3049–3053.
- [20] Huiying Li, Emily Wenger, Shawn Shan, Ben Y. Zhao, and Haitao Zheng. 2019. Piracy Resistant Watermarks for Deep Neural Networks. *arxiv:1910.01226* (2019). <https://arxiv.org/abs/1910.01226>
- [21] Meng Li, Qi Zhong, Leo Yu Zhang, Yajuan Du, Jun Zhang, and Yong Xiangt. 2020. Protecting the Intellectual Property of Deep Neural Networks with Watermarking: The Frequency Domain Approach. In *Proc. of TrustCom*. 402–409.
- [22] Shen Li, Yanli Zhao, Rohan Varma, Omkar Salpekar, Pieter Noordhuis, Teng Li, Adam Paszke, Jeff Smith, Brian Vaughan, Pritam Damania, and Soumith Chintala. 2020. PyTorch Distributed: Experiences on Accelerating Data Parallel Training. *Proceedings of the VLDB Endowment* 13, 12 (2020), 3005–3018.
- [23] Yiming Li, Yong Jiang, Zhifeng Li, and Shu-Tao Xia. 2022. Backdoor learning: A survey. *IEEE Transactions on Neural Networks and Learning Systems (Early Access)* (2022), 1–18.
- [24] Yue Li, Benedetta Tondi, and Mauro Barni. 2021. Spread-Transform Dither Modulation Watermarking of Deep Neural Network. *Journal of Information Security and Applications* 63 (2021), 103004.
- [25] Zheng Li, Chengyu Hu, Yang Zhang, and Shanqing Guo. 2019. How to prove your model belongs to you: A blind-watermark based framework to protect intellectual property of DNN. In *Proc. of ACSAC*. 126–137.
- [26] Hanwen Liu, Zhenyu Weng, and Yuesheng Zhu. 2021. Watermarking Deep Neural Networks with Greedy Residuals. In *Proc. of ICML*. 6978–6988.
- [27] Nils Lukas, Yuxuan Zhang, and Florian Kerschbaum. 2021. Deep Neural Network Fingerprinting by Conferrable Adversarial Examples. In *Proc. of ICLR*.
- [28] Erwan Le Merrer, Patrick Pérez, and Gilles Trédan. 2020. Adversarial frontier stitching for remote neural network watermarking. *Neural Computing and Applications* 32, 13 (2020), 9233–9244.
- [29] Ryota Namba and Jun Sakuma. 2019. Robust Watermarking of Neural Network with Exponential Weighting. In *Proc. of AsiaCCS*. 228–240.
- [30] Bita Darvish Rouhani, Huili Chen, and Farinaz Koushanfar. 2019. DeepSigns: An End-to-End Watermarking Framework for Ownership Protection of Deep Neural Networks. In *Proc. of ASPLOS*. 485–497.
- [31] Karen Simonyan and Andrew Zisserman. 2015. Very Deep Convolutional Networks for Large-Scale Image Recognition. In *Proc. of ICLR*.
- [32] Nitish Srivastava, Geoffrey E. Hinton, Alex Krizhevsky, Ilya Sutskever, and Ruslan Salakhutdinov. 2014. Dropout: a simple way to prevent neural networks from overfitting. *Journal of Machine Learning Research* 15, 1 (2014), 1929–1958.
- [33] Sebastian Szylinder, Buse Gul Atli, Samuel Marchal, and N. Asokan. 2021. DAWN: Dynamic Adversarial Watermarking of Neural Networks. In *Proc. of MM*. 4417–4425.
- [34] Enzo Tartaglione, Marco Grangetto, Davide Cavagnino, and Marco Botta. 2020. Delving in the loss landscape to embed robust watermarks into neural networks. In *Proc. of ICPR*. 1243–1250.
- [35] Yusuke Uchida, Yuki Nagai, Shigeyuki Sakazawa, and Shin’ichi Satoh. 2017. Embedding Watermarks into Deep Neural Networks. In *Proc. of ICMR*. 269–277.
- [36] Jiangfeng Wang, Hanzhou Wu, Xinpeng Zhang, and Yuwei Yao. 2020. Watermarking in deep neural networks via error back-propagation. *Electronic Imaging* 2020, 4 (2020), 22–1.
- [37] Siyue Wang, Xiao Wang, Pin-Yu Chen, Pu Zhao, and Xue Lin. 2021. Characteristic Examples: High-Robustness, Low-Transferability Fingerprinting of Neural Networks. In *Proc. of IJCAI*. 575–582.
- [38] Tianhao Wang and Florian Kerschbaum. 2019. Attacks on Digital Watermarks for Deep Neural Networks. In *Proc. of ICASSP*. 2622–2626.
- [39] Le Ya and Xuan Yang. 2015. Tiny imagenet visual recognition challenge. *CS 231N* 7, 7 (2015), 3.
- [40] Peng Yang, Yingjie Lao, and Ping Li. 2021. Robust Watermarking for Deep Neural Networks via Bi-level Optimization. In *Proc. of ICCV*. 14821–14830.
- [41] Hongyi Zhang, Moustapha Cissé, Yann N. Dauphin, and David Lopez-Paz. 2018. mixup: Beyond Empirical Risk Minimization. In *Proc. of ICLR*.
- [42] Jialong Zhang, Zhongshu Gu, Jiyong Jang, Hui Wu, Marc Ph. Stoecklin, Heqing Huang, and Ian M. Molloy. 2018. Protecting Intellectual Property of Deep Neural Networks with Watermarking. In *Proc. of AsiaCCS*. 159–172.